ELSEVIER

Tectonophysics 351 (2002) 255–261

TECTONOPHYSICS

www.elsevier.com/locate/tecto

Compressional wave velocity of granite and amphibolite up to melting temperatures at 1 GPa

Yoshitaka Aizawa [a,*], Kazuhiko Ito [b], Yoshiyuki Tatsumi [c]

[a] *Institute for Geothermal Sciences, Kyoto University, Noguchibaru, Beppu 874-0903, Japan*
[b] *Faculty of Business Administration, Southern Osaka University, Osaka 587-8555, Japan*
[c] *Institute for Frontier Research on Earth Evolution (IFREE), Japan Marine Science and Technology Center (JAMSTEC), Yokosuka 237-0061, Japan*

Received 7 February 2002; accepted 29 April 2002

Abstract

Compressional wave velocities (V_P) at above-solidus temperatures and at 1 GPa were obtained for a granite and amphibolite, which are considered to be major constituents of the continental crust. The temperature variation of velocities showed that the V_P values of granite decreased with rising temperature, but substantially increased beyond the melting temperature (850–900 °C). Such an increase may be caused by the $\alpha-\beta$ transition of quartz. The velocities of amphibolite decreased linearly with increasing temperature and dropped sharply at temperatures above the solidus (700 °C), indicating that partial melting of amphibolite acts to significantly lower the seismic velocities.

Keywords: Compressional wave velocity; Partial melting; Granite; Amphibolite

1. Introduction

Seismic observations have provided key information on the structure of the continental crust in the form of velocity–depth relations. In order to interpret the velocity profiles in terms of petrology, laboratory measurements of elastic properties have been conducted for a variety of rock types (e.g., Birch, 1960, 1961; Christensen, 1979; Christensen and Mooney, 1995; Ito and Tatsumi, 1995; Jackson et al., 1990; Kern et al., 1999). However, owing to technical difficulty, the effect of temperature high enough to cause partial melting on elastic wave velocities is not sufficiently understood. For instance, considering the phase relations of plausible constituents of continental crust, such as granite and amphibolite at high $P-T$ conditions corresponding to high heat flow (Lachenburch and Sass, 1977), these rocks would suffer partial melting at depths (e.g., Huang and Wyllie, 1981; Wolf and Wyllie, 1995). Therefore, although the presence of low velocity zones have been proposed in the continental crust with anomalously high heat flow (e.g., Gutenberg, 1951; Kind et al., 1996; Swenson et al., 2000), the origin of such low velocity

* Corresponding author. Present address: Institute for Study of the Earth's Interior, Okayama University, Yamada 827, Misasa 682-0193, Japan. Tel.: +81-858-43-3828; fax: +81-858-43-2184.
E-mail address: aizawa@misasa.okayama-u.ac.jp (Y. Aizawa).

0040-1951/02/$ - see front matter
PII: S0040-1951(02)00251-2

zones is still in debate. In this study, we report laboratory measurements of compressional wave velocities (V_P) at 1 GPa for granite and amphibolite at temperatures beyond the solidus (800–950 °C) in order to investigate the influence of partial melting on seismic wave velocity.

2. Experiments

The experiments were carried out using a piston-cylinder apparatus with a 24-mm inner diameter and 80-mm thickness. The assembly is shown in Fig. 1. Talc was used as the pressure-transmitting medium. Nickel tubes (each 23 mm long) placed on the top and base of a carbon heater (20 mm long), act to lower the temperature around the transducer and facilitate experiments under high temperature conditions (~ 1000 °C). The sample was wrapped in Pt foil in order to avoid direct contact between the sample and the BN sleeves. Temperature was measured with a Chromel/Alumel thermocouple and the temperature gradient across the sample was estimated to be ~ 30 °C at 1000 °C.

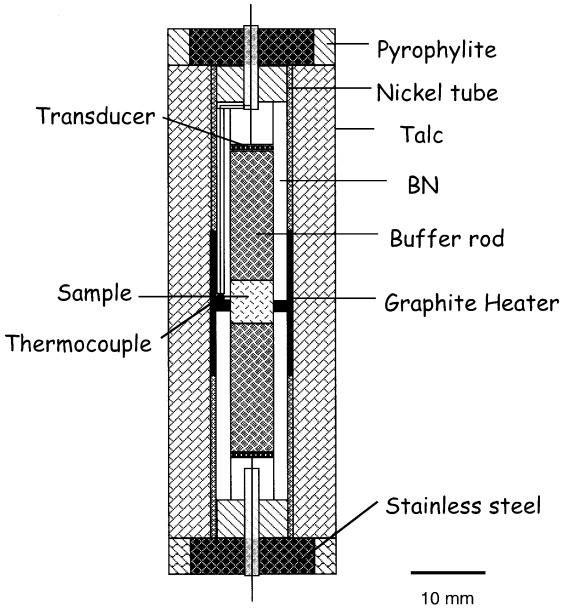

Fig. 1. The cell assembly for the velocity measurements.

$LiNbO_3$ transducers (0.5 mm thick, 36° *Y*-cut) were used to emit and receive the acoustic signals. Each transducer was mounted on the end of a platinum buffer rod. Both transmitted and reflected ultrasonic echoes were observed at the interface between the sample and the second buffer rod, and subsequently, the sample and the first buffer rod. Travel times were determined by the differences in arrival time between these echoes. Thus, the velocity determination was dependent only on the sample length and not on the buffer rods. The accuracy of each velocity measurement was better than 1%. Further details of these experiments are described in Aizawa et al. (2001).

The granite sample was collected from Nabarugawa, Osaka, Japan and mainly composed of quartz, alkali and plagioclase feldspar and biotite (Fig. 2(a)). The amphibolite sample that contains amphibole, albite and epidote is from Nikanbetsu, Hokkaido, Japan (Fig. 2(d)). The bulk rock and mineral compositions and modal compositions are shown in Table 1. The bulk chemical compositions were obtained by X-ray fluoresence spectrometers, RIGAKU Symaltics 3550 and 3070, following the procedure outlined by Goto and Tatsumi (1990). The modal compositions were estimated by mass balance calculations based on the chemical compositions of individual phases determined by an electron-probe micro-analyzer (JEOL-JXA8800). Fig. 3(a) and (b) present pole figures of the optical indicatrix (*X*, *Y*, *Z* axes) of the plagioclase and amphibole in the granite and amphibolite sample, respectively. There is no evidence for strong preferred orientation of minerals.

3. Results and discussion

3.1. Granite

Fig. 4(a) illustrates the temperature variation of the observed waveforms. Compared to previous measurements (Aizawa et al., 2001), the signals were degraded and sample echoes were slightly ambiguous, probably because the ultrasonic waves were scattered at the grain boundaries. This is probably caused by the relatively large grain size (0.3–1.5 mm) of the natural rock sample. At high temperatures, specifically immediately above the solidus (from 750 to 850 °C), the

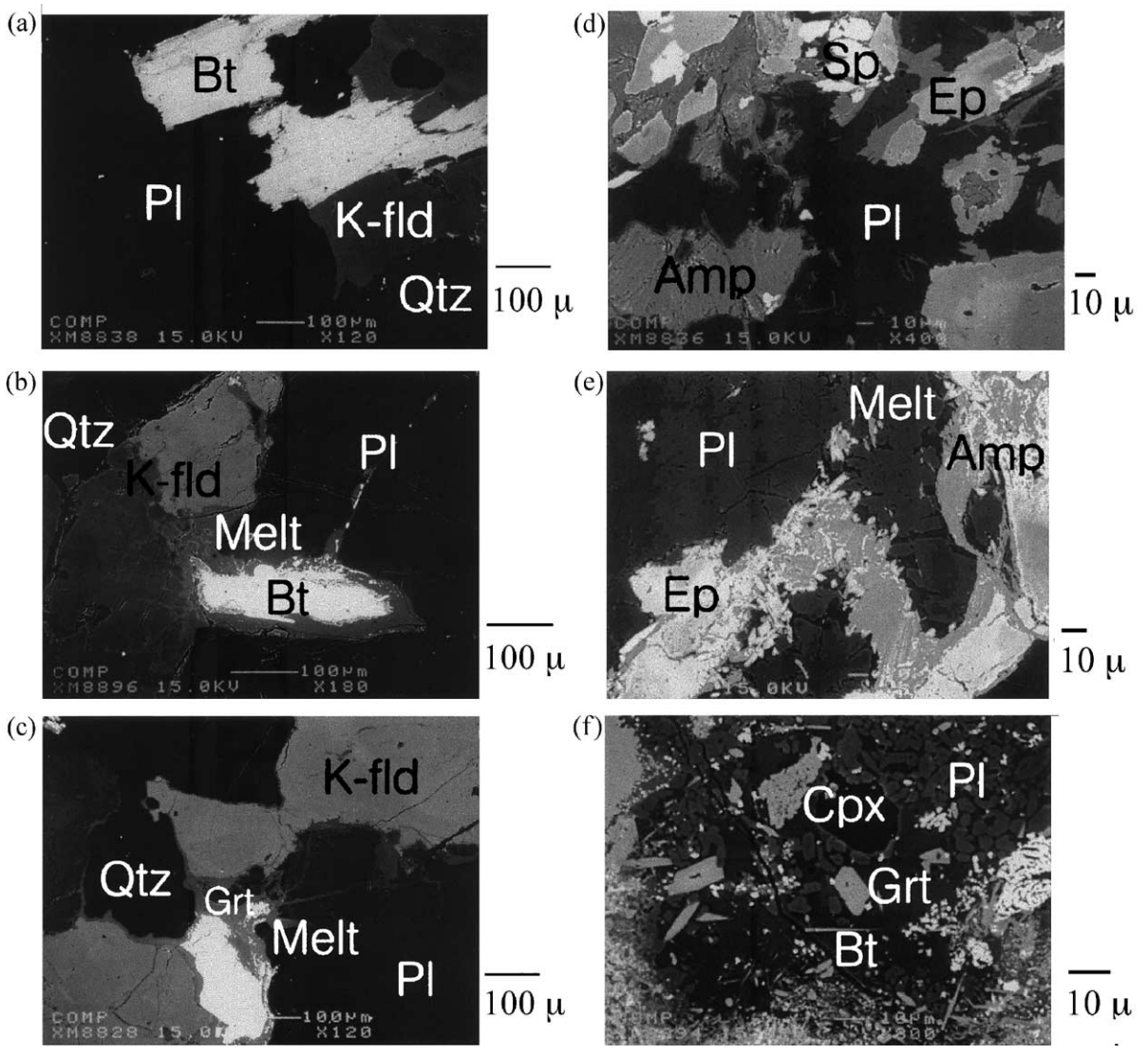

Fig. 2. Back-scattered electron images of the starting materials. (a) Granite: representative minerals are labeled (biotite (Bt), white; K-feldspar (K-f), gray; plagioclase (Pl), dark gray; quartz (Qt), black). (b) Granite at 850 °C: the melt was formed associated with the biotite breakdown reaction. The melt was observed at biotite–feldspar boundaries. (c) Granite at 970 °C: most grain boundaries are wetted by the melt. (d) Amphibolite: Amphibole (Amp), dark gray; epidote (Ep), gray; sphene (Sp), white; albite (Ab), black. (e) Amphibolite at 780 °C: the melt appears along amphibole–plagioclase grain boundaries. (f) Melt pools at 800 °C: euhedral garnet, clinopyroxene and prismatic biotite are nucleated.

amplitudes of signals decreased substantially, yielding relatively large errors in velocity determination (at most within $\pm 2\%$), though in the β-field of quartz (above 850 °C), the signals became clear again. The effect of temperature on V_P measured separately along three different directions in the granite sample is shown in Fig. 5(a).

V_P decreases substantially when the temperature approaches the $\alpha-\beta$ transition, and then increases in the β-field of quartz. The melting temperature for the

Table 1
Chemical and modal compositions of granite and amphibolite

	Granite					Amphibolite			
	Bulk	Quartz	Plagioclase	K-feldspar	Biotite	Bulk	Amphibole	Albite	Epidote
SiO_2	75.55	99.33	63.74	64.60	34.68	46.22	54.18	69.03	37.97
TiO_2	0.14	0	0	0	2.36	2.09	0.18	0	0.12
Al_2O_3	14.19	0	22.71	18.59	18.90	17.33	5.25	19.77	22.15
FeO	1.27	0	0	0.06	23.73	12.00	17.83	0.13	13.29
MnO	0.04	0	0	0	0.60	0.22	0	0.01	0.02
MgO	0.32	0	0	0	5.52	4.76	3.51	0	0
CaO	1.70	0	3.80	0.03	0	8.94	6.87	0.02	22.86
Na_2O	3.11	0	9.05	1.09	0.06	3.78	9.86	11.29	0
K_2O	3.99	0	0.08	15.05	9.62	1.00	0	0	0
Total	100.31	99.33	99.38	99.41	95.48	96.34	97.69	100.25	96.41
	mode	34.4	37.1	23.7	4.9		42.8	14.0	42.3
Oxygen		2.00	8.00	8.00	11.00		23.00	8.00	12.00
Si		1.00	2.79	2.99	2.71		8.07	3.00	3.02
Ti		0	0	0	0.13		0.04	0	0.02
Al		0	1.21	1.02	1.71		0.92	1.00	2.05
Fe		0	0	0	1.56		2.23	0	0.91
Mn		0	0	0	0.04		0	0	0
Mg		0	0	0	0.66		0.71	0	0
Ca		0	0.23	0	0		0.93	0	1.94
Na			0.73	0.10	0.01		3.09	0.97	0
K		0	0.01	0.89	0.97		0	0	0
Cation sum		1.00	4.97	5	7.79		15.98	4.97	7.94

present granite sample at 1 GPa is 750 °C, which is consistent with previous experimental works (e.g., Huang and Wyllie, 1981). The geometrical structure of partially molten rocks have been investigated in terms of dihedral angles because the relative interfacial energies between melt and grains, and between grains are supposed to control the connectivity of the melt (e.g., von Bargen and Waff, 1986; Jurewicz and Watson, 1984, 1985; Holness, 1995). Laporte (1994), however, demonstrated that significant interfacial energy anisotropies exist in quartz-bearing systems and the connectivity is influenced more by the crystallography than by the dihedral angle. The onset of melting is associated with the breakdown reactions of biotite above 750 °C, in which hydrous melt surrounding the biotite grains and garnet within the melt pools are produced. In 850 °C run, the melt is not yet completely interconnected and observed at biotite–feldspar grain boundaries (Fig. 2(b)). In 970 °C run, the melt is formed at quartz–feldspar interfaces, and intragranular feldspar melting occurs (Fig. 2(c)), and the melt is interconnected along most grain boundaries.

It should be noted that the velocity of the granite increased substantially after the transition (> 850 °C), which was well above the solidus temperature. Though the melt fraction reached about 15% at 970 °C (Fig. 2(c)), the velocities nevertheless increased, possibly associated with the crystal growth within the β-phase. It is thus suggested that partial melting of granite may even increase the seismic wave velocity at high temperatures, instead of decreasing.

3.2. Amphibolite

The temperature variations of V_P for amphibolite measured separately along the three different directions are shown in Fig. 4(b). It is well demonstrated that the first arrival transmitted and sample echoes are clearly observed. Fig. 5(b) illustrates the relationship between V_P and temperature. Here, V_P decreased linearly with temperature below 700 °C, and then dropped significantly above 700 °C. The pronounced decrease in V_P above 700 °C may be caused by the onset of partial melting. We confirmed a solidus temperature for the amphibolite of 700 °C, which is

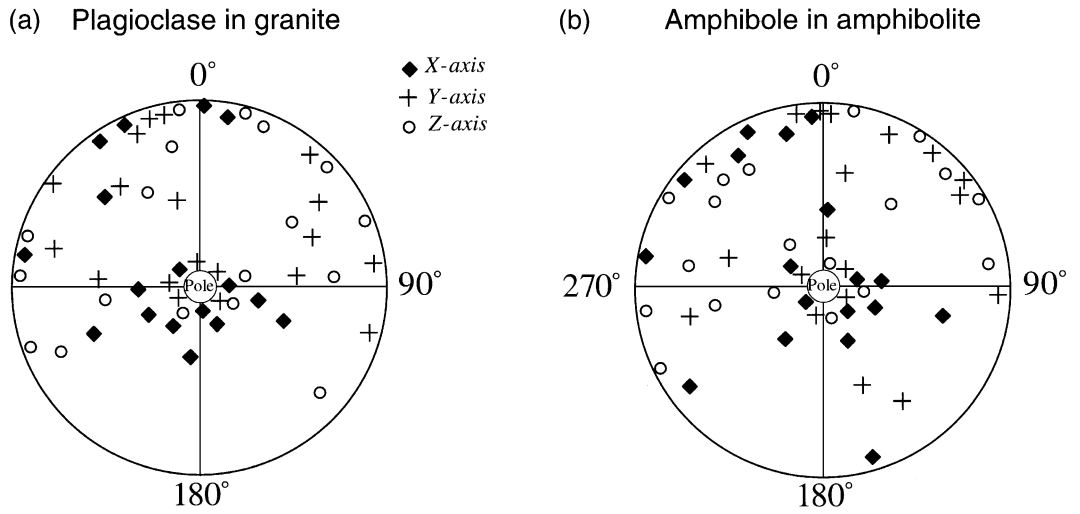

Fig. 3. The orientation of optical indicatrix (*X*-, *Y*- and *Z*-axes) of the plagioclase in granite and the amphibole in amphibolite, respectively.

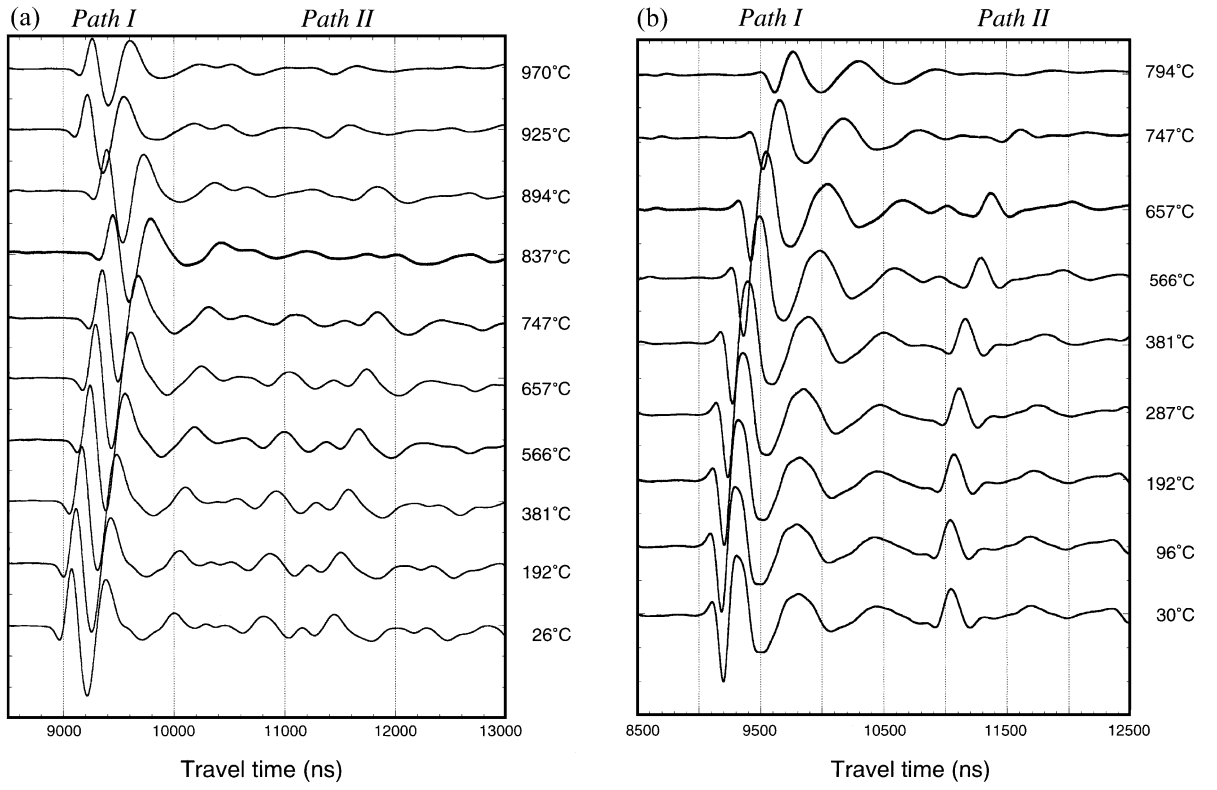

Fig. 4. Temperature variation of the observed waveforms for granite at 1 GPa and up to 970 °C (a) and for amphibolite at 1 GPa up to 794 °C (b). When the sample echo (Path II) is not sufficiently clear, we estimate the travel time by using the first arrival time (Path I).

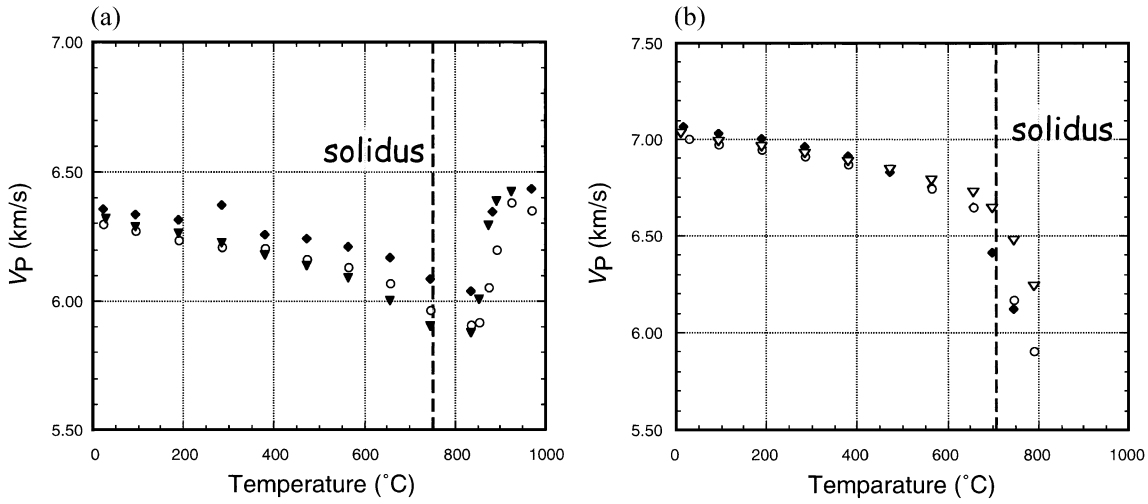

Fig. 5. Compressional wave velocity (V_P) of granite (a) and amphibolite (b) measured separately along three different directions as a function of temperature.

consistent with previous melting experiments (e.g., Wolf and Wyllie, 1995).

As discussed in the previous section, in partially melted coarser-grained solid amphibolite, the melt morphology is crystallographically controlled by the surface energy anisotropy of the hornblende-dominated system (Wolf and Wyllie, 1995). In the present experiments, melt formation along most amphibole–plagioclase boundaries leads to melt pools with angular morphologies, not the tetrahedronally shaped junctions of the interfacial energy controlled systems. In the 780 °C run, the melt comprises ~ 15% of the rock and almost surrounds the plagioclase grains (Fig. 2(e)). The melt at amphibole–plagioclase boundaries is interconnected along the rim of the amphibole grains. In the 800 °C run, the melt comprises ~ 20% of the rock. Amphibole, plagioclase and newly formed clinopyroxene, garnet and biotite are observed (Fig. 2(f)). The melt is partly associated with amphibole–plagioclase boundaries, and mostly forms through intragranular melting of plagioclase.

Compressional wave velocities of amphibolitic rocks with basaltic compositions have been measured at 0.2 and 0.6 GPa and up to 600 °C (Christensen, 1979; Kern et al., 1999). Extrapolation of these results gives V_P between about 6.7 and 6.8 km s^{-1} at 700 °C, in good agreement with the present results (Fig. 5(b)). The temperature dependence of V_P ($\delta V_P/\delta T$) is -5.4×10^{-4} km·s^{-1}·$°C^{-1}$ below the solidus (700 °C), and -5.0×10^{-3} km·s^{-1}·$°C^{-1}$ above the solidus temperature resulting in a significant reduction of seismic wave velocity due to the presence of partially molten amphibolite at depths.

4. Conclusion

The temperature variation of compressional wave velocities showed that the V_P values of granite decreased with rising temperature, but substantially increased beyond the melting temperature (850–900 °C). Such an increase may be caused by the α–β transition of quartz. The present results suggest that the presence of felsic crust with sufficiently high temperature to cause partial melting, for example, beneath southern Tibet, yield not only low seismic wave velocity but also relatively high velocity at depths, due to the quartz transition. In contrast to granite, the velocities of amphibolite decreased linearly with increasing temperature and dropped sharply at temperatures above the solidus (700 °C), indicating that partial melting of amphibolite acts to significantly lower the seismic velocities. It is likely that a significant reduction of the seismic velocity observed beneath the central Andes may be explained by the presence of partially molten amphibolite, which is

probably originated from basaltic magmas underplated at the base of the crust.

Acknowledgements

We thank Dr. T. Sano and Ms. R. Tsurudome for their help in EPMA and XRF analyses. We are grateful to Profs. S. Ji and N.I. Christensen for providing useful suggestions. This study was partly supported by Tenma Educational Institution under the Grant TEI-9602 and TEI-9702 to K. Ito.

References

Aizawa, Y., Ito, K., Tatsumi, Y., 2001. Experimental determination of compressional wave velocity of olivine aggregate up to 1000 °C at 1 GPa. Tectonophysics 339, 473–479.

Birch, F., 1960. The velocity of compressional waves in rocks to 10 kilobars, 1. J. Geophys. Res. 65, 1083–1102.

Birch, F., 1961. The velocity of compressional waves in rocks to 10 kilobars, 2. J. Geophys. Res. 66, 2199–2224.

Christensen, N.I., 1979. Compressional wave velocity in rocks at high temperatures and pressures, critical thermal gradients, and crustal low velocity zones. J. Geophys. Res. 80, 6849–6857.

Christensen, N.I., Mooney, W.D., 1995. Seismic velocity structure and composition of the continental crust: a global view. J. Geophys. Res. 100, 9761–9788.

Goto, A., Tatsumi, Y., 1990. Quantitative analysis of rocks using XRF (I). Rigaku Denki Janaru 22, 28–44.

Gutenberg, B., 1951. Crustal layers of the continents and oceans. Geol. Soc. Amer. Bull. 62, 427–440.

Holness, M.B., 1995. The effect of feldspar on quartz–H_2O–CO_2 dihedral angles at 4 kbar, with consequences for the behavior of aqueous fluids in migmatites. Contrib. Mineral. Petrol. 118, 356–364.

Huang, W.L., Wyllie, P.J., 1981. Phase relationships of S-type granite with H_2O to 35 kbar: muscovite granite from Harney Peak, South Dakota. J. Geophys. Res. 86, 10515–10529.

Ito, K., Tatsumi, Y., 1995. Measurement of elastic wave velocities in granulite and amphibolite having identical H_2O-free bulk compositions up to 850 °C at 1 GPa. Earth Planet. Sci. Lett. 133, 255–264.

Jackson, I., Rudnick, R.L., O'Reilly, S.Y., Bezant, C. 1990. Measured and calculated elastic wave velocities for xenoliths from the lower crust and upper mantle. Tectonophysics 173, 207–210.

Jurewicz, S.R., Watson, E.B., 1984. Distribution of partial melt in a felsic system: the importance of surface energy. Contrib. Mineral. Petrol. 85, 25–29.

Jurewicz, S.R., Watson, E.B., 1985. The distribution of partial melt in a granitic system: the application of liquid-phase sintering theory. Geochim. Cosmochim. Acta 49, 1109–1122.

Kern, H., Gao, S., Jin, Z., Popp, T., Jin, S., 1999. Petrophysical studies on rocks from the Dabie ultrahigh-pressure (UHP) metamorphic belt, Central China: implications for the composition and delamination of the lower crust. Tectonophysics 301, 191–215.

Kind, R., et al., 1996. Evidence from earthquake data for a partially molten crustal layer in southern Tibet. Science 274, 1692–1694.

Lachenburch, A.H., Sass, J.H. 1977. Heat flow and the thermal regime of the crust. In: Heacock, J.G. (Ed.), The Earth's Crust: Its Nature and Physical Properties. Geophys. Monogr. Ser., vol. 20. AGU, Washington, DC, pp. 626–675.

Laporte, D., 1994. Wetting behavior of partial melts during crustal anatexis: the distribution of hydrous silicic melts in polycrystalline aggregates of quartz. Contrib. Mineral. Petrol. 116, 486–499.

Swenson, J.L., Beck, S.L., Zandt, G., 2000. Crustal structure of the Altiplano from broadband regional waveform modelling: implications for the composition of thick continental crust. J. Geophys. Res. 105, 607–621.

von Bargen, N., Waff, N.S., 1986. Permeabilities, interfacial areas and curvatures of partially molten system: results of numerical computations of equilibrium microstructures. J. Geophys. Res. 91, 9261–9276.

Wolf, M.B., Wyllie, P.J., 1995. Liquid segregation parameters from amphibolite dehydration melting experiments. J. Geophys. Res. 100, 15611–15621.